

## Grow a Backbone: Bending Mechanics of Biomimetic Intervertebral Joints

Adrienne Dunk<sup>1, 2</sup>

Marine Environment Research Experience

Fall 2012

<sup>1</sup>Friday Harbor Laboratories, University of Washington, Friday Harbor, WA 98250

<sup>2</sup>Program in Environmental Sciences, Northwestern University, Evanston, IL 60208

Contact Information:

Adrienne Dunk

Program in Environmental Sciences

Northwestern University

2145 Sheridan Rd

Evanston, IL 60208

[Adriennedunk2013@u.northwestern.edu](mailto:Adriennedunk2013@u.northwestern.edu)

*Keywords: centra, morphology, intervertebral joint, moment, force*

## **Abstract**

There is huge variation in vertebral centra morphology both within and among classes. While research has noted and described these differences in detail, it has not adequately explored how centrum shape affects joint stiffness. My research explored how the existing variation between fish and mammal vertebral centra affects the loading and deflection of the intervertebral joint under homologous conditions of size and materials. I expected that bending forces would be proportionally related to the volume of intervertebral material as affected by intervertebral distance and centra morphology.

To test the stiffness of the joint, I made multiple motion segments of ABS plastic using silicone as the intervertebral material. Each centrum had a different angle of concavity, flat face, or convexity mimicking fish, land mammals and marine mammals, respectively. The Material Testing System deflected the motion segment measuring the force required at the end of a moment arm. Land and aquatic mammals create statistically similar bending moments that are distinct from all of the fish inspired designs, which are all statistically similar to each other. The trends within these findings raise more questions about how concavity and intervertebral length affect stiffness, stress, moment, and overall bending performance with biomechanic and evolutionary implications.

## **Introduction**

A key characteristic of modern vertebrates, which evolved in four independent lineages: elasmobranchii, actinopterygii, dipnoi, and tetrapoda, is a segmented vertebral column (Porter and Long, 2010). This vertebral column consists of a series of centra, which are the large bony parts of vertebrae that support the arches (Gál, 1993). As

calcified centra formed on the axis of the notochord in early fish, it created intervertebral joints, which concentrate bending forces in a smaller area increasing flexural stiffness (Liew et al., 2007). The evolutionary consequences of centra are joint formation and carangiform swimming. These lead to an increase in force transmission to the caudal fin, a stiffer body, which allows for greater acceleration, faster steady swimming, (Koob and Long, 2000) and an overall increase in swimming performance (Porter and Long, 2010). Additionally, the change from the single long beam of the notochord to multiple smaller components of the vertebral column decreases the likelihood of failure from bending. Bending creates a moment between the short elements of the beam where flexion occurs (Laerm, 1976). The heterogeneous properties of the vertebral column facilitate this bending scheme with the intervertebral material having significantly less rigidity than the calcified centra.

The function of the backbone is to transfer force created in the body out to the environment resulting in locomotion. This transfer occurs because of controlled body deformations made possible in many vertebrates by species-specific complex ligament systems linking multiple vertebrae together across joints (Koob and Long, 2000, Long et al., 1997). The backbone also transmits force via its connections to the lateral musculature and through regional morphological differences in the vertebral centra (Long, 1992). The rotational axis of an organism runs through the intervertebral discs and centra increasing the flexibility and ability of the system to transmit force. More specific bending processes and vertebral structures are also species-specific (Gàl, 1993).

The centra face morphologies vary across species from the amphicoelous, or biconid, shape of most fishes to the platyan, or flat, terrestrial mammalian shape. Aquatic

mammal's centra have slightly convex faces (Hildebrand, 1974). A motion segment, consisting of an intervertebral disc and its two adjacent centra, models the system interactions of a joint (Porter and Long, 2010). During bending, the connected surface area between an intervertebral disc and centra decreases to a theoretical single point. As the area decreases, stress increases. Ligamentous mechanisms distribute this stress across multiple centra, increasing surface contact during bending and decreasing stress in a single motion segment (Pierce et al., 2011; Laerm, 1976). The articular capsule and other features of vertebra, such as the arches, work to bind the intervertebral joint and limit movement (Gàl, 1993). These movement and binding mechanisms limit unnecessary movement in the joint while decreasing and distributing stress.

No clear understanding of how motion segment morphology affects the stiffness of the vertebral system exists. While stiffness and force transmission have garnered a lot of attention, we do not understand the impact of centra shape and intervertebral distance as well. I aim to elucidate the effect of centra morphology during bending ranging from the convex centra of cetaceans and pinnipeds through the flat faced centra of terrestrial vertebrates and multiple concave centra modeled after fish. I also explore how the length of the intervertebral disc, and therefore the total volume of intervertebral material, effects stiffness. Further, I will examine how the angle of deflection changes the moment created. Based upon Buchholtz findings linking increased intervertebral length with increased flexion, I hypothesize that with increased concavity and increased intervertebral disc length stiffness will decrease because of an increase in total intervertebral material (2001). For increased angles of deflection, I hypothesize an increased moment as this is the usual pattern in physics.

## Methods

### *Vertebral Centra Design*

To model the possible range of centra shapes in fishes, land mammals, and aquatic mammals I designed vertebral centra with differing levels of concavity and convexity in Google SketchUp. To isolate the morphology of the centra face, each centrum was the same height at 30 mm tall and 26 mm in diameter. I measured the cup angle at the center of the centrum. The five morphologies tested were a 90° angle with a depth of 13 mm, a 120° angle with a depth of 7.5 mm, a 150° angle with a depth of 3.5 mm, an 180° angle with no height change, and a 210° angle with a 3.5 mm protrusion (Fig 1). I only designed angles on one face so that when assembled there was a flat surface on either end to attach to the mounting block and moment arm.

### *Intervertebral Joint Construction*

Once designed, I printed the centra out of ABS plastic on a MakerBot Industries Thing-O-Matic 3-D Printer. I assembled one set of motion segments each with a 7 mm, 10 mm, and 13 mm intervertebral distance measured between the rims of the two centra. The material used was semi-permanent 3M Marine Sealant Silicone. I assembled these motion segments in PVC pipe that I cut in half and lubricated so the silicone would not stick to the mold. After filling the matching centra with the intervertebral material and closing the mold, excess material exited via a hole in the side of the mold (Fig 2). The silicone motion segments then required between four and seven days to dry depending on the volume of material. I inset the moment arm for testing by drilling a hole into the end of one centrum per motion segment and gluing the seam.

### *Testing Procedure and Data Collection*

For testing, I mounted each motion segment separately onto a wooden tee. Protruding from the opposite end of the motion segment was a moment arm aligned with the Synergie 100 Material Testing System (MTS). The MTS completed a single cyclic testing regime for each treatment putting the intervertebral joint under tension of displacement to 0.95°, 1.90°, or 2.85° and then returned to zero five times. I recorded the force at each known deflection resulting in ten force data points per test, five during extension and five during returning. Because of bounce in the system, displacement and force recordings often went below zero. To account for this, the data was re-zeroed by averaging the negative forces for the trial and adding that value onto the recorded force measurement. I only used adjusted force measurements for calculations and graphing.

### *Data Analysis*

To test for significance of each variable, I ran a two way ANOVA (JMP Pro9, SAS Institute). This test compared force, measured directly from testing, and moment defined as:

$$M = F \cdot l \quad (1)$$

Where F is the force measured and l is the distance from the center of the motion segment to the crosshead of the MTS. Moment is a better measurement for this test because it is more easily comparable across future testing methods. These two data sets were compared across the three treatments of morphology (5 cases), intervertebral length (3 cases), and angle of displacement (3 cases). I also ran student t-tests to test for statistical

similarity between the cases within each treatment (JMP Pro9, SAS Institute). To compare two variables across each case of the third treatment, I looked at the moment at displacement of intervertebral length for each morphological change, and the moment created at different angles of displacement across all morphologies for each given intervertebral length.

Additional inquiry looked at the work and work per volume of intervertebral material across each intervertebral length and morphology. Work is calculated as:

$$W = F*d \quad (2)$$

where F is the force measured and d is the distance the crosshead displaced the moment arm. I also looked at moment per angle of displacement versus angle of displacement for each morphology to see how the force requirement changed during bending. The final comparison was of work lost per morphology found by taking the difference between the volume of work put into the system during extension and that regained during returning.

## Results

The force and resultant moment, when compared across all three treatments, were statistically significant ( $F_{3, 446} = 131.34218$ ,  $p < 0.0001$ ;  $F_{3, 446} = 132.1839$ ,  $p < 0.0001$ ). The first treatment, centra morphology, (Fig. 4A, B) indicated that morphologies 1 and 2, the convex and flat centra, were statistically similar to each other and different from morphologies 3, 4, and 5, the three concave centra which were similar to each other ( $F_{4, 445} = 9.5055$ ,  $p < 0.0001$ ;  $F_{4, 445} = 9.6359$ ,  $p < 0.0001$ ). The second treatment, variable

intervertebral length, showed statistical difference between each length for both the force and moment (Fig. 4C, D). Surprisingly, the intermediate intervertebral length of 10 mm required the least force and moment compared against the adjacent lengths of 7 mm and 13 mm across all morphologies and displacements ( $F_{2, 447} = 50.5150$ ,  $p < 0.0001$ ;  $F_{2, 447} = 49.0537$ ,  $p < 0.0001$ ). The final treatment (Fig. 4E-F) found a statistical difference between each displacement angle measured across all morphologies and intervertebral lengths ( $F_{2, 447} = 135.0449$ ,  $p < 0.0001$ ;  $F_{2, 447} = 137.2297$ ,  $p < 0.0001$ ).

Morphologies 1, 3, and 5 exhibited a decrease in moment at the 10 mm intervertebral length (Fig. 5A, C, E). Morphology 2, however, showed a continual increase in moment across all displacement angles and intervertebral lengths (Fig 5B). Morphology 4 was the only centra to show a mixed pattern. For the two larger displacement angles, the moment decreased across all three intervertebral lengths, but it increased between the 7 mm and 10 mm length and then decreased at 13 mm (Fig. 5D). No theory unites these trends.

For the 10 mm intervertebral length, moment increased linearly with displacement angle (Fig. 6A-E). The slope of the line formed by angle of displacement versus moment is the flexural stiffness of the motion segment. This increase of moment with increased displacement was statistically significant across all morphologies though its magnitude indicates no clear pattern ( $F_{6, 143} = 433.4378$ ,  $p < 0.0001$ ). Morphology 3, 150° concave, ( $F_{2, 27} = 193.0315$ ,  $p < 0.0001$ ) had the lowest moment and stiffness. Morphology 4, 120° concave, ( $F_{2, 27} = 258.9215$ ,  $p < 0.0001$ ) consistently had a large moment and stiffness (Fig. 6C, D). The remaining morphologies had no correlation between the stiffness and the magnitude of the moment (Fig 6A, B, E).

For intervertebral lengths of 10 mm and 13 mm, there was a statistical difference between the work ( $F_{3, 446} = 347.1975$ ,  $p < 0.0001$ ) and for all intervertebral lengths there was a statistical difference between work per volume ( $F_{3, 446} = 273.2753$ ,  $p < 0.0001$ ) measured across all three displacements for each morphology (Fig 7). At an intervertebral length of 7 mm, the work remained similar across all the morphologies while the work per volume exhibited a significant continued decrease ( $F_{4, 145} = 20.8136$ ,  $p < 0.0001$ ) as concavity increased (Fig 7 A, B). At 10 mm intervertebral length, it required the least work to bend the joints with morphology 3 requiring the least overall ( $F_{4, 145} = 10.6314$ ,  $p < 0.0001$ ). The work per volume also decreased significantly as the morphologies became more concave ( $F_{4, 145} = 17.8707$ ,  $p < 0.0001$ ) (Fig C, D). The work decreased across the intermediate morphologies with a 13 mm intervertebral length ( $F_{4, 145} = 9.6950$ ,  $p < 0.0001$ ) as did the work per volume ( $F_{4, 145} = 16.0650$ ,  $p < 0.0001$ ) (Fig E, F).

The expected results for the angle of displacement versus the moment per angle of displacement were straight lines, as the moment should be constant for a unit of displacement despite the total displacement. This, however, was not the result for four of five morphological treatments (Fig. 8). All of the centra treatments except for 120° concave exhibited a statistically significant (210:  $F_{2, 87} = 6.1060$ ,  $p = 0.0033$ ; 180:  $F_{2, 87} = 4.5976$ ,  $p = 0.0126$ ; 150:  $F_{2, 87} = 3.6218$ ,  $p = 0.0308$ ; 90:  $F_{2, 87} = 5.2576$ ) decrease as the angle of displacement increased. This trend indicates that it was hardest to bend the motion segment initially, but that it became easier once it had been bent initially.

The most efficient morphology depended on the displacement. By measuring the work lost by each morphology under two different deflection regimes, we got different

patterns. At  $1.90^\circ$  displacement of motion segments with a 7 mm intervertebral disc there was a clear cubic pattern with the minimum work lost occurring at  $135^\circ$  concave (Fig 9A). At  $0.95^\circ$  deflection of the same motion segments, the pattern was clearly a fourth power function with a minimum work lost at the intermediate morphology of  $195^\circ$  convex (Fig 9B).

## **Discussion**

I measured the moment required to bend a motion segment under the three treatments: intervertebral length, angle of displacement, and centra morphology. These treatments were bio-inspired from variations present across and within many taxa and phylum. The combinations of these treatments resulted in forty-five specific treatments with one replication of each test.

### *Evolutionary Implications*

Mammal centra were statistically different from fish centra with mammals creating a larger moment during bending (Fig 4 A, B). For terrestrial mammals, this increased moment may have to do with the efficiency with which they transfer thrust to the medium of air as opposed to water. Aquatic mammals may be able to maintain this increased moment that fish cannot because of an increased energy budget. Mammals are positively buoyant for ease of feeding and have an inexpensive air acquiring method, surface breathing. Cetaceans also have the highest stiffness (Fig 6 A) which may help them maintain such a large body; however, this may be a derived difference, as I did not model the rest of the vertebral mechanisms such as arches and soft tissue processes.

Further, the bending moment per unit displacement decreased significantly as the degree displacement increased for all morphologies except 120° concave (Fig 8). This trend may show a preference for small bending angles as the increased moment would transfer more force into locomotion.

The efficiency dependence on deflection angle indicates that morphology may have adapted to aid swimming styles that are dependent on the environment (Fig 9). As environmental factors changed, they may have made swimming by a particular axial angular displacement more advantageous, and centra morphology mutated accordingly. The efficiency of bending, viewed as least work lost, is dependent on intervertebral length, morphology, and angle of displacement. An area of further study is how the frequency of bending affects force and efficiency.

### *Terrestrial Mammals*

Morphology 4, the flat centra, represented a common terrestrial mammalian vertebral design conserved across orders (Gål, 1993). This morphology best fit my hypothesis with results showing that increased deflection and intervertebral length increased the bending moment in near linear relationships (Fig. 5B). This platyan shape had an intermediate stiffness, which fits with other research indicating that the size and shape of the vertebrae in mammals is less of a factor than the surrounding processes. Terrestrial mammals have multiple ways to resist flexion. Monkeys and wallabies rely on the *ligamenta flava* compared to cats such as jaguars and tigers for which the intervertebral disc resists bending. Further, in these models mobility was independent of

the size of the motion segment of bones used, (Gàl, 1993) so it follows that this motion segment did not function at the extremes of mechanical testing.

### *Aquatic Mammals*

Aquatic mammals, pinnipeds and cetaceans, have vertebral centra ranging from platyan to convex within a spinal column. The convex morphology is statistically similar across force and moment to the flat morphology (Fig 4 A, B), but is statistically different in stiffness (Fig 6 A, B). This agrees with findings that relate stiffness and force to the bending and thrust creation centers of the body.

Within the pinniped clade, there are three families. Each of these families utilizes a different swimming style ranging from pelvic to pectoral oscillations. When comparing these locomotion methods to vertebral morphology, the linear length was the most indicative dimension. The longer and wider a centrum proportionally was, the stiffer the joint (Pierce et al., 2011). These propulsive regions also coincide with findings of slight, though unmeasured, convexity on the centra face (Gàl, 1993).

This same stiffness theory applies to cetaceans, which swim dorso-ventrally using fluke oscillation paired with body displacement anterior of the fluke, increasing stride length. The increased stiffness created by elongated and convex centra is especially clear at the fluke-torso junction and acts to increase the wave amplitude relative to the body size of the whale. The initiated wave is subtle, but the wave experienced at the fluke is significantly larger (Buchholtz, 2001).

Research indicates that the intervertebral disc length increases in the pre-caudal and caudal region that increases vertebral displacement (Buchholtz, 2001). My results

match this (Fig 5A) showing an increase in moment between the minimum and maximum intervertebral lengths at all displacement angles.

### *Fishes*

Fishes limit the direction of vertebral flexion to lateral motion (Laerm, 1967). To support repetitive axial bending, fishes developed complex tendon, bone, muscle, and skin systems that transmit force down the body axis while decreasing stress on the rest of the body. These systems, along with the morphology of the motion segment should affect the stiffness of the bending moment and therefore determine the work needed to create an external moment (Long et al., 1997). Our preliminary research did not find any statistical difference between the morphology of the three concave cases in either force or moment (Fig 4 A, B) to support this previous research.

When angular stiffness of the system increases, the bending amplitude at a joint creates proportional bending further down the spine. Variation in angular stiffness correlates with structural variation of the centra and the length of the anterior centrum in a motion segment (Long, 1992). The structural variation of fish centra depends on the length, width, and depth of the total structure, and the steepness of the concavity within the faces of the centra (Laerm, 1967). Our findings did not show a specific trend between angular stiffness and increased concavity (Fig 6 C-E). The average degree of concavity had the most stiffness while the least concave had the lowest stiffness of any model making an overarching conclusion impossible.

### *Future Work*

These findings did not fit with current theories of how the motion segment should behave across the morphologies or intervertebral length indicating that more research is required to elucidate the mechanisms behind the varied results. Future work should include more replications of each treatment so that testing conditions such as silicone dry time have no impact on the results. Additionally, the procedure should change so that data gathering occurs after the joint cyclically bends multiple times to reflect biological conditions (Long, 1992). Motion segments should also be tested in different deflection angle orders so that there is no cyclic weakening as the joint gets bent repeatedly in previous tests.

The tests should be repeated in multiple materials and at differing frequencies to clarify the processes at play and to better mimic biological conditions. Finally, the motion segments could be redesigned to account for the lateral shape of vertebrae and the corresponding spongy bone.

An interesting implication of this research is how ontogenetic change effects fish vertebrae. Fish exhibit indeterminate growth that is possible because fish centra have an “open” growth scheme meaning that the centra can elongate at the rim of the amphicoel over the entire course of the organism’s life. This may change the steepness of the centrum concavity (Nordvik et al., 2005). An interesting foray would be to relate the concavity of the centra with the developmental phase of a fish and explore how the axial bending dynamics correlate with the overall physical interactions of that fish and the environment.

## Acknowledgements

I thank Adam Summers, Marianne Porter, and Stephanie Crofts for their guidance in designing and executing my experiment. I thank Lauren Trotta, Bryson Albrecht, Gavin Brackett, Todd Sigley, and Jessica Blanchette for ensuring my physical safety while working in the student shop and helping to secure materials. I especially thank Lauren Trotta and Bryson Albrecht for their everlasting exuberance when reviewing my findings.

## Literature Cited

- Buchholtz, E. A.**, (2001). Vertebral osteology and Swimming Style in Living and Fossil Whales (Order: Cetacea). *Journal of Zoology*. **253**, 175-190.
- Gal, J. M.**, (1993). Mammalian Spinal Biomechanics: II. Intervertebral Lesion Experiments and Mechanisms of Bending Resistance. *Journal of Experimental Biology*. **174**, 281-297.
- Hildebrand, M.** (1974). Body Skeleton: Structure and Development of Vertebrae. In *Analysis of vertebrate structure*. pp 157 - 170. New York: Wiley.
- Koob, T. J., Long, J. H. Jr.**, (2000). The Vertebrate Body Axis: Evolution and Mechanical Function. *American Zoologist*. **40**, 1-18.
- Laerm, J.**, (1976). The Development, Function, and Design of Amphicoelous Vertebrae in Teleost Fishes. *Zoological Journal of the Linnean Society*. **58**, 237-254.
- Liew, C. W., Root, R. G., Long, J. H. Jr., Koob, T. J.**, (2007). Using Artificial Organisms To Study The Evolution of Backbones in Fish. *Proceedings of the 2007 IEEE Symposium on Artificial Life*, 108-114.
- Long, J. H. Jr.**, (1992). Stiffness and Damping Forces in the Intervertebral Joints of Blue Marlin, (*Makaira nigricans*). *Journal of Experimental Biology*. **162**, 131-155.
- Long, J. H. Jr., Pabst, D. A., Shepherd, W. R., McLellan, W. A.**, (1997). Locomotor Design of Dolphin Vertebral Columns: Bending Mechanics and Morphology of *Delphinus delphis*. *Journal of Experimental Biology*. **200**, 65-81.

**Nordvik, K., Kryvi, H., Totland, G. K., Grotmol, Sindre G.,** (2005). The Salmon Vertebral Body Develops through Mineralization of Two Preformed Tissues that are Encompassed by Two Layers of Bone. *Journal of Anatomy*. **206**, 103-114.

**Pierce, S. E., Clack, J. A., Hutchinson, J. R.,** (2011). Comparative Axial Morphology in Pinnipeds and its Correlaation with Aquatic Locomotory Behaviour. *Journal of Anatomy*. **219**, 502-514.

**Porter, M. E., Long, J. H. Jr.,** (2010). Vertebrae in Compression: Mechanical Behavior of Arches and Centra in the Gray Smooth-Hound Shark (*Mustelus californicus*). *Journal of Morphology*. **271**, 366-375.

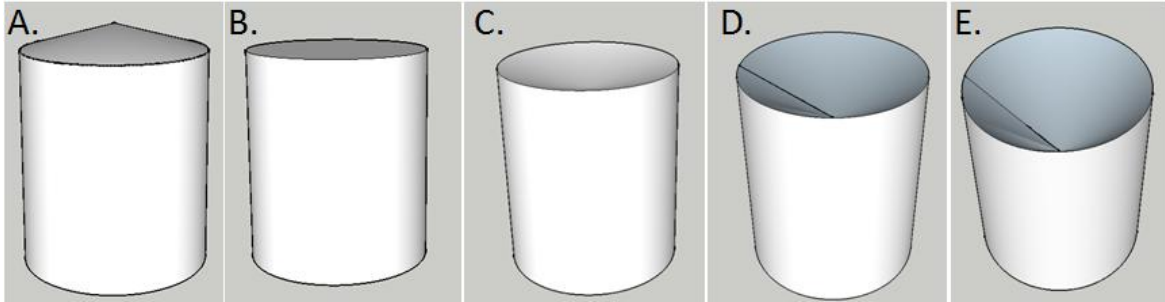


Figure 1. Computer rendered 3-D models of vertebral centra from Google Sketch-Up. (A) Test morphology 1. Convex model measured at  $210^{\circ}$  at center. (B) Test morphology 2. Flat surface measured at  $180^{\circ}$  at center. (C) Test morphology 3. Concave model measured at  $150^{\circ}$  at the center. (D) Test morphology 4. Concave model measured at  $120^{\circ}$  at the center. (E) Test morphology 5. Concave model measured at  $90^{\circ}$  at the center.

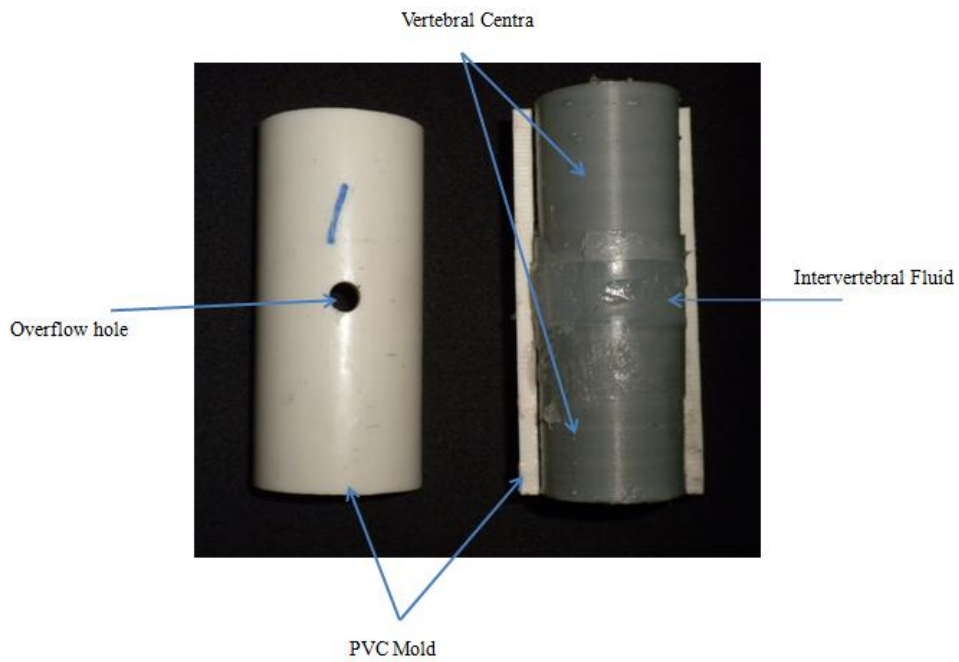


Figure 2. Open mold with dried motion segment. The motion segment is assembled in the PVC mold and the excess material exits via the overflow hole. After the material has dried, the mold is opened and the motion segment removed.

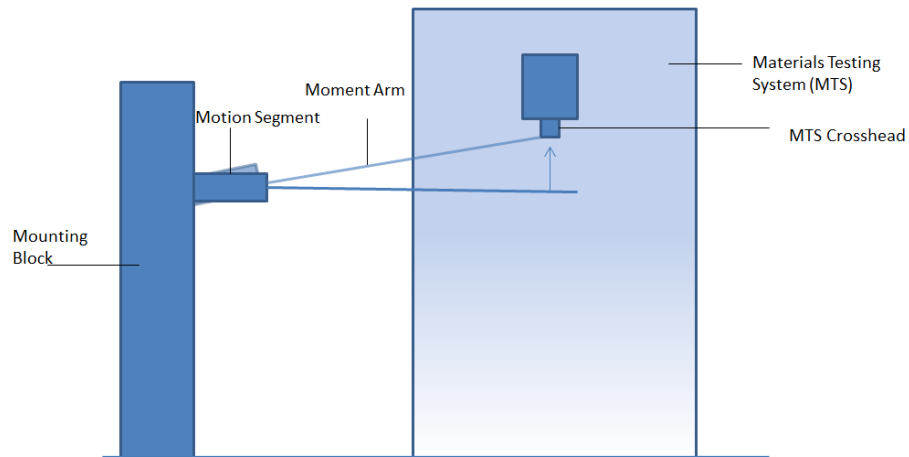


Figure 3. Testing set-up. The motion segment, consisting of an intervertebral disc and the two adjacent centra, is mounted such that one centrum is immovable and the other has the moment arm extending from it. The MTS crosshead grips the far end of the moment arm and moves upwards a set distance, bending the motion segment and measuring the force necessary for displacement. For testing, we used a cyclic bending test where the MTS lifted and returned the crosshead and therefore joint five times at each designated deflection.

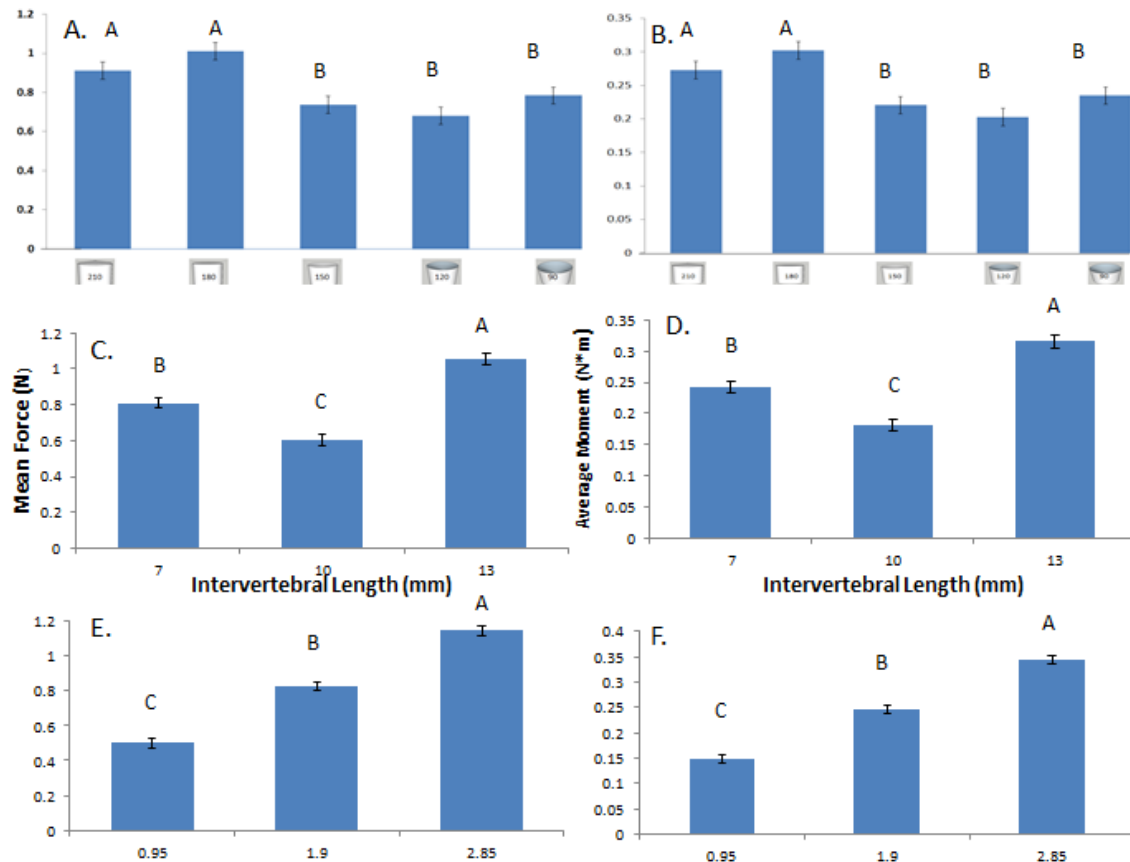


Figure 4: Effects on average force and moment by centra morphology, intervertebral distance, and angle of displacement. Force measurements significant under all variables ( $F_{3, 446} = 131.34218$ ,  $p < 0.0001$ ). Moment measurements significant under all variables ( $F_{3, 446} = 132.1839$ ,  $p < 0.0001$ ). (A) Average Force and Centra Morphology. Morphologies 1 and 2, the convex and flat centra are statistically similar to each other and different from morphologies 3, 4, and 5, the concave centra which are all statistically alike ( $F_{4, 445} = 9.5055$ ,  $p < 0.0001$ ). (B) Average Moment and Centra Morphology. This shows the same trends as panel A ( $F_{4, 445} = 9.6359$ ,  $p < 0.0001$ ). (C) Average Force and Intervertebral Length. Each length is statistically different ( $F_{2, 447} = 50.5150$ ,  $p < 0.0001$ ). (D) Average Moment and Intervertebral Length. This shows the same trend as panel C ( $F_{2, 447} = 49.0537$ ,  $p < 0.0001$ ). (E) Average Force and Angle of Displacement. Each displacement angle is statistically different ( $F_{2, 447} = 135.0449$ ,  $p < 0.0001$ ). (F) Average Moment and Angle of Displacement. This panel shows the same trend as panel E ( $F_{2, 447} = 137.2297$ ,  $p < 0.0001$ ).

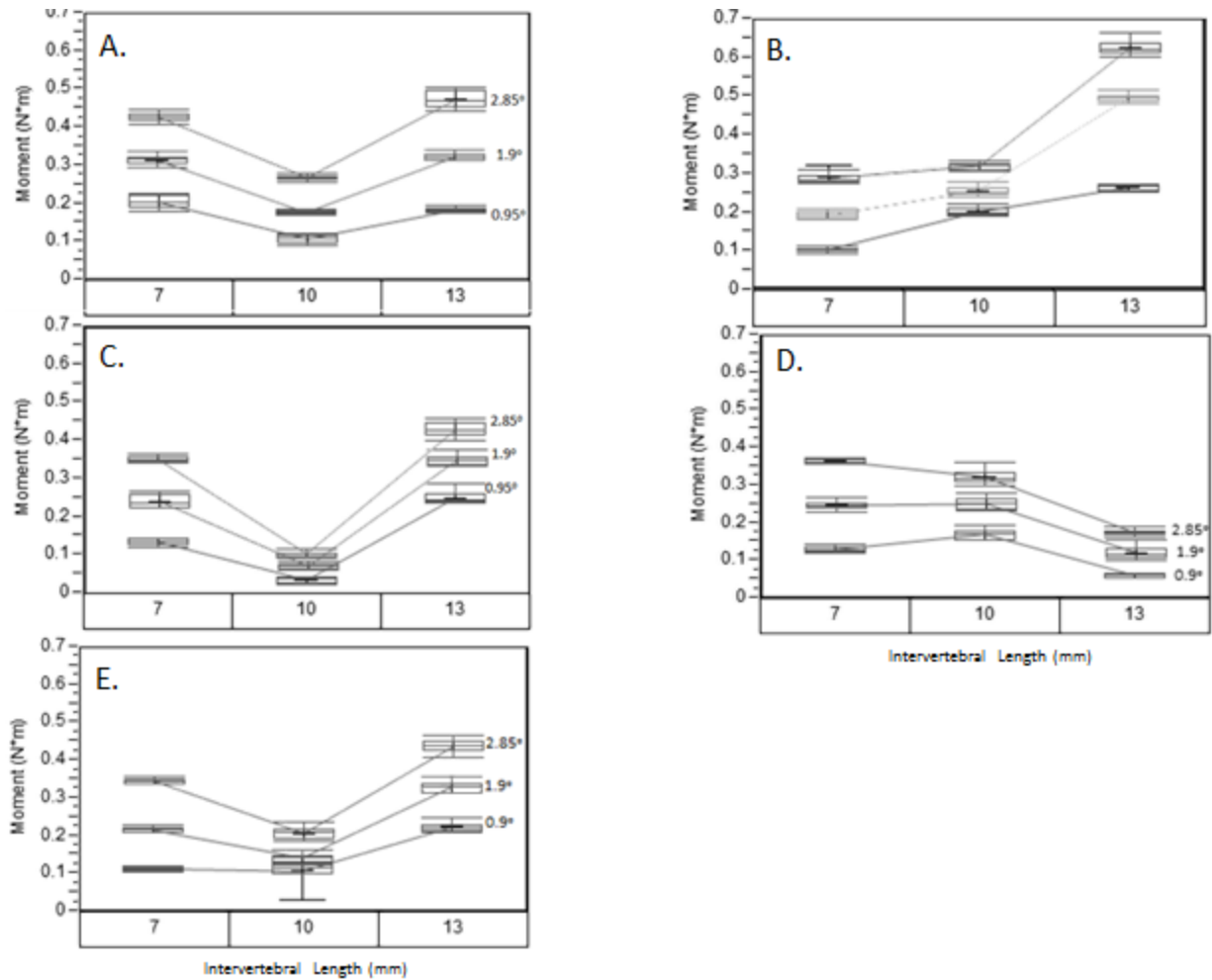


Figure 5: Moment created by different intervertebral lengths at each displacement angle. Each box represents 10 data points. (A) Morphology 1, 210° Convex, shows the lowest moment at an intervertebral spacing of 10 mm across all displacement angles. (B) Morphology 2, 180° flat, shows an increase in moment at each displacement though none of the increases shows a linear relationship. (C) Morphology 3, 150° concave, shows a marked low in moment at an intervertebral length of 10 mm across all displacements. (D) Morphology 4, 120° concave, shows a nonlinear decrease as the intervertebral length increased across displacement angles of 2.85° and 1.9° but at 0.9°, the moment increases with an increase in length from 7 mm to 10 mm before decreasing at 13 mm.

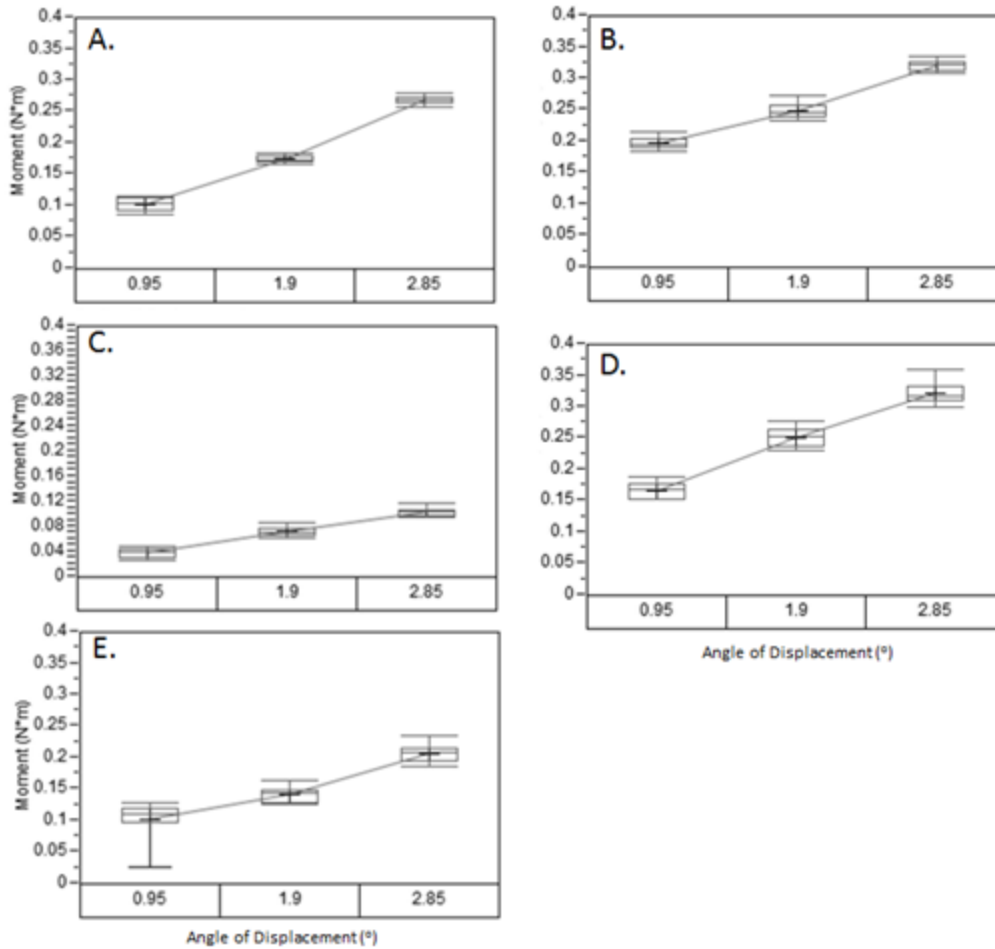


Figure 6: Differences across centra morphology in the angle of displacement per average moment for 10 mm intervertebral length ( $F_{6, 143} = 433.4378$ ,  $p < 0.0001$ ). (A) Morphology 1,  $210^\circ$  centra has the highest stiffness measured at  $0.087 \text{ Nm}^2$ , but only creates an intermediate moment ( $F_{2, 27} = 1115.376$ ,  $p < 0.0001$ ). (B) Morphology 2,  $180^\circ$  centra has an intermediate stiffness at  $0.065 \text{ Nm}^2$  and created a larger moment ( $F_{2, 27} = 346.2855$ ,  $p < 0.0001$ ). (C) Morphology 3,  $150^\circ$  concave created the least moment and had the lowest stiffness at  $0.034 \text{ Nm}^2$  ( $F_{2, 27} = 193.0315$ ,  $p < 0.0001$ ). (D) Morphology 4,  $120^\circ$  centra has a high stiffness at  $0.0820 \text{ Nm}^2$  and a created the largest moment ( $F_{2, 27} = 258.9215$ ,  $p < 0.0001$ ). (E) Morphology 5,  $90^\circ$  concave centra had a low stiffness at  $0.055 \text{ Nm}^2$  and moment ( $F_{2, 27} = 70.2896$ ).

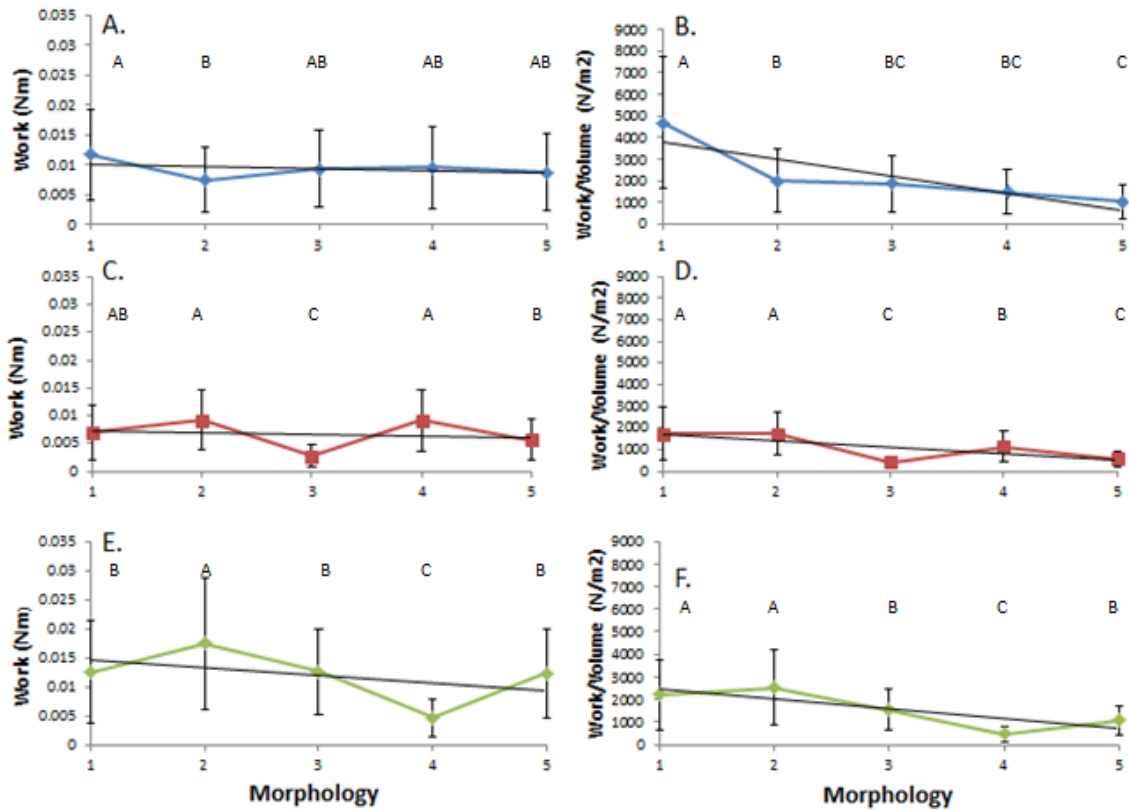


Figure 7: Differences in the Work ( $F_{3, 446} = 347.1975$ ,  $p < 0.0001$ ) and Work per Volume ( $F_{3, 446} = 273.2753$ ,  $p < 0.0001$ ) of the five tested vertebral morphologies across all displacements. (A) The work done by each morphology with a 7 mm intervertebral length remained the same and was not significant (B) At 7 mm intervertebral length, the work per volume decreased as the concavity of the morphology increased ( $F_{4, 145} = 20.8136$ ,  $p < 0.0001$ ). (C) At a 10 mm intervertebral length, the work differed significantly across each morphology ( $F_{4, 145} = 10.6314$ ,  $p < 0.0001$ ). (D) The work per volume at 10 mm decreased across each morphology as the volume increased ( $F_{4, 145} = 17.8707$ ,  $p < 0.0001$ ). (E) At 13 mm, the work decreased across the three intermediate morphologies ( $F_{4, 145} = 9.6950$ ). (F) The work per volume decreased more steeply than the work did across all of the morphologies ( $F_{4, 145} = 16.0650$ ,  $p < 0.0001$ ).

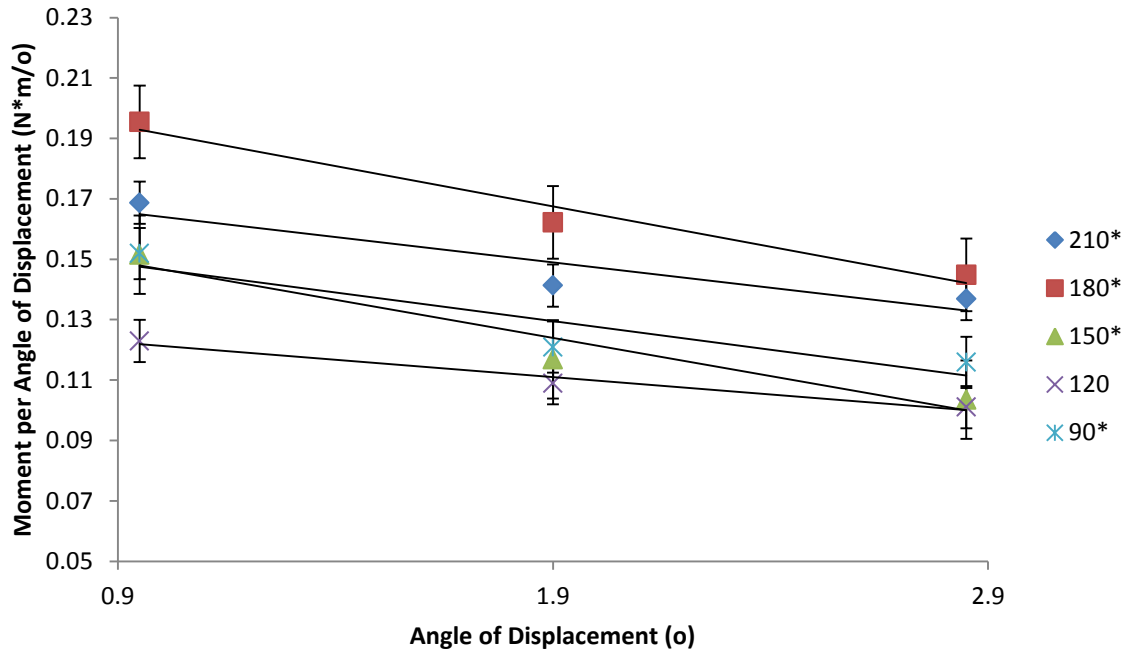


Figure 8: Angle of displacement versus the moment per displacement angle across each of the five morphologies.  $N = 30$  for each point graphed. The asterisk next to the legend denotes statistical significance. As the angle of displacement increased, the moment per degree displacement decreased (210:  $F_{2, 87} = 6.1060$ ,  $p = 0.0033$ ; 180:  $F_{2, 87} = 4.5976$ ,  $p = 0.0126$ ; 150:  $F_{2, 87} = 3.6218$ ,  $p = 0.0308$ ; 90:  $F_{2, 87} = 5.2576$ ).

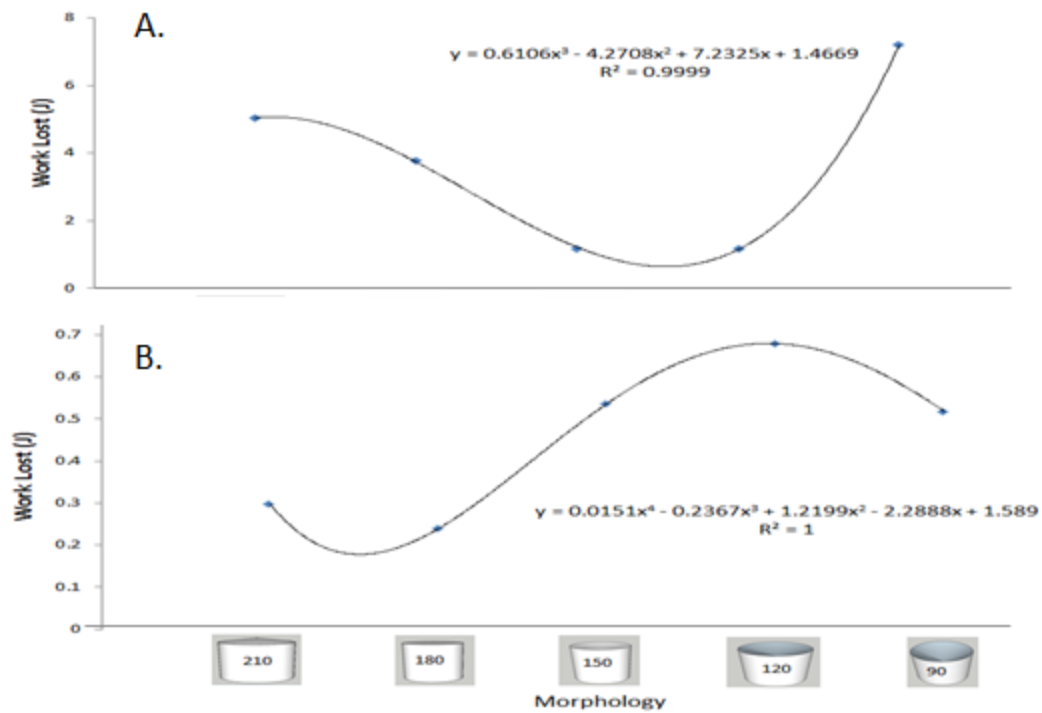


Figure 9: Work lost during cycle 3 of cyclic testing of morphology with 7 mm intervertebral length. (A) Work lost at cyclic displacement of  $1.90^\circ$ . Trend fits a cubic function with a minimum around  $135^\circ$  concave. (B) Work lost at cyclic displacement of  $0.95^\circ$ . Trend fits a polynomial function to the fourth with a minimum around  $195^\circ$  convex.